

# AN EXPLICIT UNIVERSAL GATE-SET FOR EXCHANGE-ONLY QUANTUM COMPUTATION

M. HSIEH<sup>1</sup>, J. KEMPE<sup>1,2,3</sup>, S. MYRGREN<sup>1</sup> AND K. B. WHALEY<sup>1</sup>

ABSTRACT. A single physical interaction might not be universal for quantum computation in general. It has been shown, however, that in some cases it can achieve universal quantum computation over a subspace. For example, by encoding logical qubits into arrays of multiple physical qubits, a single isotropic or anisotropic exchange interaction can generate a universal logical gate-set. Recently, encoded universality for the exchange interaction was explicitly demonstrated on three-qubit arrays, the smallest nontrivial encoding. We now present the exact specification of a discrete universal logical gate-set on four-qubit arrays. We show how to implement the single qubit operations exactly with at most 3 nearest neighbor exchange operations and how to generate the encoded controlled-NOT with 27 parallel nearest neighbor exchange interactions or 50 serial gates, obtained from extensive numerical optimization using genetic algorithms and Nelder-Mead searches. We also give gate-switching times for the three-qubit encoding to much higher accuracy than previously and provide the full specification for exact *CNOT* for this encoding. Our gate-sequences are immediately applicable to implementations of quantum circuits with the exchange interaction.

## 1. INTRODUCTION

To implement universal computation in the quantum regime, one must be able to generate any unitary transformation on the logical qubit states. By now it has become part of the quantum computation folklore that the group  $SU(2)$  of single-qubit operations and an entangling two-qubit operation such as the controlled-NOT (*CNOT*) can generate any unitary transformation exactly [1, 2]. Furthermore it has been shown that there are *discrete* universal elementary gate-sets which approximate any unitary transformation with arbitrary precision efficiently<sup>1</sup> (see [3, 4] for details). One such set is comprised of  $\{H, \frac{\pi}{8}, CNOT\}$  [5], where  $H$  is the Hadamard transform and  $\frac{\pi}{8}$  is a phase gate, both acting on a single qubit. In this sense,  $H$ ,  $\frac{\pi}{8}$  and *CNOT* comprise a quantum analogue to a classical *universal logical gate-set*.

---

*Date:* October 29, 2018.

<sup>1</sup>We use *efficient* in the computational sense, meaning that we can implement the transformation with a number of elementary gates polynomial in the number of qubits. Note that not all general unitary transformations can be implemented efficiently; in fact the generic unitary transformation on  $n$  qubits requires an exponential amount of elementary gates. Our usage of *efficient* here means that given there is a sequence of one- and two-qubit gates that generates  $U$  then we can approximate this  $U$  to arbitrary accuracy with a sequence of gates drawn from our elementary set and such that we only have polynomial overhead in the number of gates used. Further, to double the precision we only need a constant amount of additional gates. This is the notion we need to define efficient computation.

The traditional paradigm of quantum computation of “one physical qubit = one logical qubit” is often hard to implement because in the presently known menu of physical implementation schemes, it is usually difficult to control at least one of either the single-body or the two-body operations [6].

A prime example is the Heisenberg interaction (with Hamiltonian  $H_E^{i,j} = J_{ij} \vec{S}_i \otimes \vec{S}_j$  between spin particles  $i$  and  $j$ , where  $\vec{S}_i = \frac{1}{2} \vec{\sigma}^i$  and  $\sigma_{x,y,z}^i$  are the usual Pauli matrices acting on qubit  $i$ ). It has many attractive features [7, 8] that have led to its being chosen as the fundamental two-qubit interaction in a large number of recent proposals: Its functional form is very accurate — deviations from the isotropic form of the interaction, arising only from relativistic corrections, can be very small in suitably chosen systems. It is a strong interaction, so that it should permit very fast gate operation, well into the GHz range for several of the proposals. At the same time, it is very short ranged, arising from the spatial overlap of electronic wavefunctions, so that it should be possible to have an on-off ratio of many orders of magnitude. We will assume that the interaction can be switched on and off between coupled qubits [8]. Unfortunately, the Heisenberg interaction by itself is not a universal gate, in the sense that it cannot generate any arbitrary unitary transformation on a collection of spin-1/2 qubits. So, every proposal has supplemented the Heisenberg interaction with some other means of applying independent one-qubit gates (which can be thought of as time-dependent local magnetic fields). But the need to add this capability to the device adds considerably to the complexity of the structures, by putting unprecedented demands on “g-factor” engineering of heterostructure materials [9, 10], requiring that strong, inhomogeneous magnetic fields be applied, or involving microwave manipulations of the spins that may be slow and may cause heating of the device. These added complexities may well exact a high cost, perhaps degrading the quantum coherence and clock rate of these devices by several orders of magnitude.

*Encoded universality* [11] provides a way around this problem in some crucial cases, for example when the “easy” interaction is the exchange interaction, by entirely eliminating the need for single-body physical operations. By encoding each logical qubit in an array of multiple physical qubits, sequences of two-body nearest-neighbor exchange interactions are sufficient to generate the logical  $SU(2)$  and  $CNOT$  operations<sup>2</sup> on the encoded qubits [14, 11, 15] and single-spin operations and all their attendant difficulties can be avoided.

One drawback of the theory of encoded universality [14] is that it establishes the sufficiency of certain two-body interactions for universality in a non-constructive way, not offering explicit methods with which to specify the sequences of physical implementable Hamiltonians corresponding to the encoded logical gates. In particular it is not clear at the outset how many physical interactions are required to implement each of the logical gates in some layout of the qubits. Encoded computation schemes are only viable if the number of physical interactions to be applied to

---

<sup>2</sup>Note that it has been shown that a *generic* two-qubit interaction alone generates universal computation [12, 13]. However, by an irony of nature most implementable interactions in current quantum computation schemes happen to fall in the set of exceptions to this. These exceptions include the ubiquitous exchange interaction (both isotropic and anisotropic) and several other interactions that exhibit a certain amount of symmetry, which makes them *non-generic* in the above sense. Even for interactions that fall into the category of being universal by themselves, explicit gate-constructions have to be found in a case by case basis.

the qubits is not too large, where the threshold is determined by currently achievable decoherence and switching times. In most cases, numerical methods are the only way to find explicit sequences of Hamiltonians for a set of universal gates for some realistic arrangement of the physical qubits. Recently, more or less explicit universal logical gate-sets have been given for a three-qubit encoding using only the exchange interaction [16], for the  $XY$ -interaction [6] and for the generalized anisotropic exchange Hamiltonian [17]. In [16] an initial encoding of three physical qubits per logical qubit is used and a sequence of 19 Hamiltonians is presented that implements the encoded  $CNOT$ . However this  $CNOT$  is given up to local unitary operations only, and the encoded single-qubit operations are given in terms of Euler-angle rotations for the group  $SU(2)$ . Some further processing is needed to obtain a universal discrete gate-set, needed to implement quantum circuits *in terms of the computational basis* [18].

We present here a complete scheme for universal quantum computation on four-qubit encodings in a one- (or two-)dimensional layout with nearest neighbor interactions only. We specify the encoding and layout and give all the gate switching times to obtain the encoded  $H$ ,  $\frac{\pi}{8}$  and  $CNOT$  in the computational basis without further post-processing. This scheme provides an immediately applicable building block for exchange-only quantum circuits. We also provide new gate sequences for the  $CNOT$  in the three-qubit encoding to higher precision and with different symmetries than in [16] and provide the complete set of gates for the exact encoded  $CNOT$  in this smaller encoding. Although the four-qubit encoding has a slightly larger overhead in spatial resources than the three-qubit encoding it offers several advantages. A quantum computation begins by setting all encoded qubits to the (logical) zero state. In our scheme this state is a tensor product of singlet states. This state is easily obtained using the exchange interaction: if a strong  $H_{12}$  is turned on in each coded block and the temperature made lower than the strength  $J$  of the interaction, these two spins will equilibrate to their ground state, which is the singlet state. Unlike the smaller three-qubit encoding we do not require here any additional weak magnetic fields for initialization. This aspect renders the four-qubit encoding particularly attractive. Another advantage is that the four-qubit scheme is conceptually simpler for use in quantum logic when the properties of robustness to noise are also taken into account. Whereas the four-qubit logical states constitute a decoherence free subspace (DFS) under collective decoherence [14], the three-qubit logical states constitute a decoherence free subsystem in which the logical state evolution is defined by only one component of the tensor product space. A third advantage of the four-qubit encoding is that additional protection against single qubit errors can be achieved in this case by control of extra exchange interactions to form a supercoherent qubit [19].

The structure of this paper is as follows. First, we describe the four-qubit encodings which define our logical space and give the physical layout of the qubits. We then specify the Hamiltonians required to generate the single-qubit operations and the  $CNOT$  gate on the encoded qubits. The numerical methods used to obtain the exchange gate sequence for the encoded  $CNOT$  and further details are described in Appendices A and B. The same numerical methods are used to obtain new high accuracy gate sequences for the exact  $CNOT$  in the three-qubit encoding. We conclude with a brief discussion of a solid-state implementation scheme

in which these results can be readily applied, and some open problems meriting further consideration.

## 2. FOUR-QUBIT ENCODING

We define the logical zero-state and one-state on one encoded qubit as

$$(1) \quad |0_L\rangle = \frac{1}{2} (|01\rangle - |10\rangle) \otimes (|01\rangle - |10\rangle)$$

$$(2) \quad |1_L\rangle = \frac{1}{\sqrt{3}} (|t_+\rangle \otimes |t_-\rangle - |t_0\rangle \otimes |t_0\rangle + |t_-\rangle \otimes |t_+\rangle),$$

where  $|t_0\rangle = \frac{1}{\sqrt{2}} (|01\rangle + |10\rangle)$ ,  $|t_-\rangle = |00\rangle$ , and  $|t_+\rangle = |11\rangle$ . For a more detailed discussion on how to obtain these encodings, refer to [11, 15]. To initialize a computation all logical qubits have to be prepared in the  $|0_L\rangle$  state. Note that here the  $|0_L\rangle$  state is a tensor product of singlets  $\frac{1}{\sqrt{2}}(|01\rangle - |10\rangle)$ . As detailed in the previous section this will be advantageous in many experimental settings since it will permit easy initialization of the logical qubits at the beginning of a computation.

The arrays are spatially configured to permit serial nearest-neighbor exchanges between the physical qubits in a one-dimensional layout:

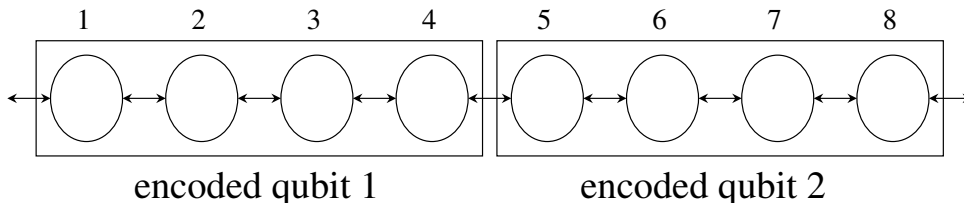


FIGURE 1. Serial configuration of eight physical qubits comprising a system of two encoded qubits.

We could also imagine these qubit arrays in a two-dimensional layout, where several of the one-dimensional layers are stacked on top of each other. Our construction of gate sequences will also hold for the two-dimensional setting. It suffices to note that the only difference is that along the layers of arrays the fourth qubit of each array is coupled to the first qubit of the next, whereas between layers the first qubit of one array in one layer is interacting with the first qubit of an array in the other. But note that both encoded states  $|0_L\rangle, |1_L\rangle$  are symmetric with respect to swapping qubit 1 with qubit 4 and qubit 2 with qubit 3, so we obtain exactly the same gate-sequence for *CNOT* for a coupling of the two first qubits of an array - all we need to do is to relabel the qubits on the bottom array as 4, 3, 2, 1.

The basis states of the logical space defined by two encoded qubits are  $|0_L0_L\rangle, |0_L1_L\rangle, |1_L0_L\rangle$  and  $|1_L1_L\rangle$ .

## 3. SINGLE-QUBIT OPERATIONS

Our goal is to construct the single-qubit Hadamard  $H$  and  $\frac{\pi}{8}$  gates, defined as

$$(3) \quad \frac{\pi}{8} = e^{i\pi/8} \begin{pmatrix} e^{-i\pi/8} & 0 \\ 0 & e^{i\pi/8} \end{pmatrix}, \quad H = \frac{1}{\sqrt{2}} \begin{pmatrix} 1 & 1 \\ 1 & -1 \end{pmatrix}.$$

on the encoded qubits, using a sequence of exchange interactions  $H_E^{i,i+1} = \frac{J_{i,i+1}}{4}(\sigma_x^i \sigma_x^{i+1} + \sigma_y^i \sigma_y^{i+1} + \sigma_z^i \sigma_z^{i+1})$  on adjacent pairs of physical qubits  $i$  and  $i + 1$ . The matrices  $\sigma_{x,y,z}^i$  are the usual Pauli matrices acting on the  $i$ th qubit and  $J_{i,i+1}$  is the coupling constant. When we write  $H_E^{i,i+1}$  we assume that the Hamiltonian acts on the  $i$ th and  $i + 1$ st qubit as specified and as the identity on all the other qubits. For convenience we are going to add a multiple of the identity to  $H_E$  (which just gives an unobservable global phase), and work with the rescaled interaction

$$(4) \quad E^{i,i+1} = \frac{1}{2}(\sigma_x^i \otimes \sigma_x^{i+1} + \sigma_y^i \otimes \sigma_y^{i+1} + \sigma_z^i \otimes \sigma_z^{i+1} + I^i \otimes I^{i+1}) = \begin{pmatrix} 1 & 0 & 0 & 0 \\ 0 & 0 & 1 & 0 \\ 0 & 1 & 0 & 0 \\ 0 & 0 & 0 & 1 \end{pmatrix}.$$

so that  $\exp(-i(J_{ij}/\hbar)t\bar{S}_i \cdot \bar{S}_j) \equiv \exp(-i(J_{ij}/2\hbar)tE^{i,j})$  (up to a global phase). We will give all exchange times in units of  $2\hbar/J_{ij}$  [7].

Consider the effect of two particular exchanges on the logical states of a single encoded qubit. First, we note that in the code-subspace the action of the exchange  $E^{1,2}$  is equal to that of  $E^{3,4}$ , with both of these generating the transformation  $|0_L\rangle \rightarrow -|0_L\rangle$  and  $|1_L\rangle \rightarrow |1_L\rangle$ . So  $-E^{1,2}$  is equivalent to a  $\sigma_z$  operation on a single logical qubit. Therefore the Hamiltonian for the encoded  $\frac{\pi}{8}$  operation, up to an unobservable global phase, is exactly  $e^{i\frac{\pi}{8}E^{1,2}}$ .

Next, consider the exchange  $E^{2,3}$ . The action of this in the code-space is equivalent to  $E^{1,4}$ . The effect of the  $E_{23}$  operation on a single logical qubit is:

$$(5) \quad E^{2,3} = \begin{pmatrix} \frac{1}{2} & \frac{\sqrt{3}}{2} \\ \frac{\sqrt{3}}{2} & -\frac{1}{2} \end{pmatrix}.$$

By examining the effect of the  $E^{1,2}$  and  $E^{2,3}$  operations on the code-space, we can obtain an exact encoded Hadamard operation as  $H = e^{it_1 E^{1,2}} e^{it_2 E^{2,3}} e^{it_1 E^{1,2}}$ , where  $t_1 = \frac{1}{2} \arcsin \sqrt{\frac{2}{3}} = 0.4777$  and  $t_2 = \arccos \sqrt{\frac{1}{3}} = 0.9553$ .

The exact specifications of exchange operations for these single qubit gates are depicted in Fig. 2.

#### 4. ENCODED *CNOT* OPERATION

To obtain the encoded *CNOT* we used numerical methods and proceeded in two stages. In the first step we attempted to obtain a gate  $U_{cnot}^{exchange}$  that is *equivalent* to the encoded *CNOT* up to local unitary transformations on the encoded qubits.  $U_{cnot}^{exchange}$  is *locally equivalent* to *CNOT* if there are single-qubit unitary operations  $U_1, U_2, V_1, V_2$  (acting on the first and second encoded qubit, respectively) such that

$$(6) \quad CNOT = (U_1 \otimes U_2) U_{cnot}^{exchange} (V_1 \otimes V_2)$$

In the second stage we numerically obtained the local unitary operations  $U_1, U_2, V_1, V_2$  to get from  $U_{cnot}^{exchange}$  to the real *CNOT* in the computational basis and to obtain the gate-sequences of exchange interactions corresponding to each of these local operations  $U_i, V_i, i = 1, 2$ . The reason for splitting the task into these two stages is the following. A result by Makhlin [20] shows that all locally equivalent gates are characterized by only three real parameters,  $M_1$  (a complex number) and  $M_2$  (real), which we will refer to as the *Makhlin-invariants* in what follows. Appendix A gives

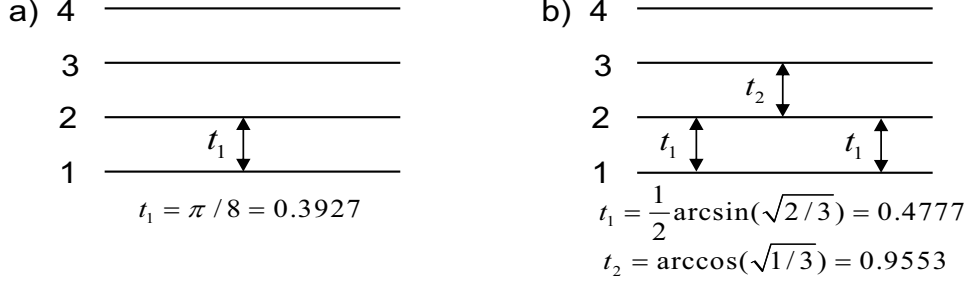


FIGURE 2. a) One exchange interaction is sufficient to generate the encoded  $\frac{\pi}{8}$  gate. b) three nearest neighbor exchanges allow to generate the encoded Hadamard gate. The  $t$  values are the time parameters corresponding to the individual exchanges with  $t = \pi/8 = 0.3927$ ,  $t_1 = 0.4777$  and  $t_2 = 0.9553$ . All times are given in units of  $2\hbar/J_{ij}$ .

a brief summary of how  $M_1$  and  $M_2$  are calculated. For the *CNOT*,  $M_1 = 0$  and  $M_2 = 1$ . The reduction to three parameters greatly simplifies the numerical search and allowed us to obtain the gate sequences by a combination of genetic algorithms [21] and Nelder-Mead simplex searches [22, 23]. The Makhlin invariants give rise to a simple fitness function  $f = \|M_1(\text{CNOT}) - M_1(\text{Candidate})\| + \|M_2(\text{CNOT}) - M_2(\text{Candidate})\|$ , where  $\|\cdot\|$  is the complex norm. A gate sequence that generates a value  $f = 0$  is therefore equivalent to a *CNOT*.

It is imperative for successful quantum computation over a subspace that any permissible operation over the encoded qubits must act unitarily on linear combinations of these basis states and not “leak” any amplitude out of the subspace into its complement and vice versa. We will capture this requirement by defining a *leakage parameter*  $\Lambda$ . Then any permissible two-qubit physical operation  $W$  must keep the code-subspace invariant, i.e. obey the following equation<sup>3</sup>:

$$(7) \quad \Lambda = 4 - \sum_{s=0}^1 \sum_{t=0}^1 \sum_{u=0}^1 \sum_{v=0}^1 |\langle s_L t_L | W | u_L v_L \rangle|^2 = 0.$$

If leakage occurs  $\Lambda > 0$ . We note that any  $W$  that is locally equivalent to *CNOT* or any other unitary logical operation over two encoded qubits must *by definition* generate a leakage parameter of  $\Lambda = 0$ . However, we have found through numerical inspection that the search space in this problem is heavily pocked with local minima in which the Makhlin invariants are close to the desired values for *CNOT*, but which “leak” out of the logical space by generating a  $\Lambda$  value larger than 0. In our numerical searches, we overcame this problem by defining our fitness function as  $\mathcal{F} = f + \Lambda$ , optimizing explicitly for not only a Makhlin invariant match, but also for non-leakage.

<sup>3</sup>Note that exchange operations *within* an array of 4 qubits keep the one-qubit code space invariant and do not leak. Leakage can only occur when we couple two arrays (see [14] for details).

A detailed description of our search algorithms and of the accuracy of our gate sequence can be found in Appendix B.

For a gate  $U_{cnot}^{exchange}$ , locally equivalent to the  $CNOT$ , we found a gate sequence of 34 nearest neighbor exchange interactions. Figure 3 and Table 1 show the layout and time parameters.

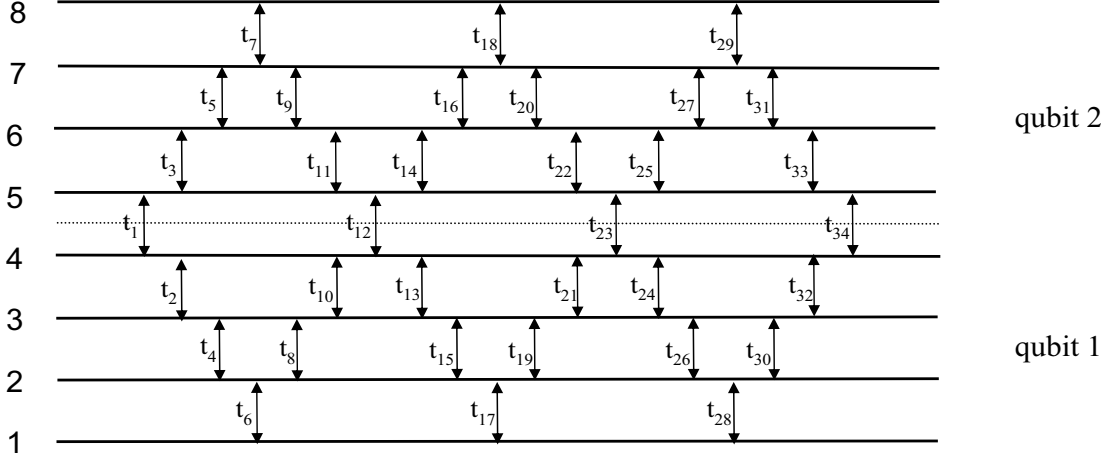


FIGURE 3. Gate sequence of 34 exchange interactions for the encoded  $CNOT$ , with the corresponding time parameters, given in Table 1.

Exchange Time	Qubit 1	Qubit 2	Times	Exchange Time	Qubit 1	Qubit 2	Times
$t_1$	4	5	1.90680	$t_{18}$	7	8	0.95629
$t_2$	3	4	1.59536	$t_{19}$	2	3	1.06260
$t_3$	5	6	1.26290	$t_{20}$	6	7	0.68131
$t_4$	2	3	1.59745	$t_{21}$	3	4	0.59800
$t_5$	6	7	2.06920	$t_{22}$	5	6	1.19942
$t_6$	1	2	0.05331	$t_{23}$	4	5	1.04719
$t_7$	7	8	0.76951	$t_{24}$	3	4	3.14138
$t_8$	2	3	1.59747	$t_{25}$	5	6	0.95529
$t_9$	6	7	0.71337	$t_{26}$	2	3	1.63957
$t_{10}$	3	4	1.59958	$t_{27}$	6	7	1.91303
$t_{11}$	5	6	1.26287	$t_{28}$	1	2	2.47920
$t_{12}$	4	5	1.90667	$t_{29}$	7	8	2.18627
$t_{13}$	3	4	0.59810	$t_{30}$	2	3	1.05736
$t_{14}$	5	6	1.71467	$t_{31}$	6	7	0.94814
$t_{15}$	2	3	1.06264	$t_{32}$	3	4	3.14170
$t_{16}$	6	7	0.91559	$t_{33}$	5	6	4.09690
$t_{17}$	1	2	2.30240	$t_{34}$	4	5	2.09434

TABLE 1. Gate switching times for the sequence of 34 exchange interactions of Figure 3, given in units of  $2\hbar/J$ .

Note that those exchanges that are on a vertical line in Figure 3 involve disjoint sets of qubits and can be applied *in parallel*, where each cycle of gates lasts as long as the longest switching time in the set of parallel gates. If we count the number of parallel operations, we obtain 19 gate cycles.

In the second stage we searched for the encoded local unitary gates  $U_1, U_2, V_1, V_2$  (see Eq. (6)) that transform the 34-gate sequence into an exact *CNOT* on the computational basis states, Eqs. 1 and 2. It has been shown previously [15, 16] that each encoded local unitary can be obtained by a sequence of four exchange gates. We employ here the nearest neighbor layout as shown in Figure 4. The constructions in [15, 16] involve non-nearest neighbor interactions, with  $E_{13}$  instead of  $E_{23}$ . It is easy to see, however, that replacing  $E_{13}$  with  $E_{23}$  in the arguments of [15, 16] also leads to a sequence of four exchanges.

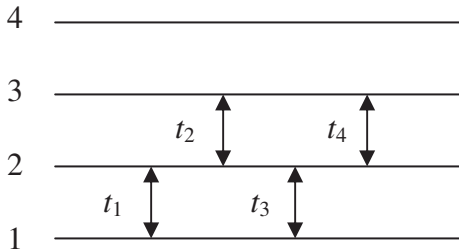


FIGURE 4. Local unitaries can be generated using a sequence of 4 exchange gates as shown.

These 16 remaining gates (4 for each local unitary) can be obtained either as the result of numerical optimization of a suitable cost function, or from solving the system of non-linear equations derived from the element-wise equivalency condition between the objective matrix and the product of the four exchange matrices. We employed the optimization approach using a Nelder-Mead simplex search because of its high efficiency and generality. A similar approach has been used in [18], where the cost function (a combination of a matrix distance between the actual gate and the desired gate and a non-leakage requirement) and the details of our numerical search calculations can be found. To reduce the probability of sampling only local minima, we sampled a large number (5 million) of randomly selected initial points in parameter space. We were able to determine the four local unitaries and their corresponding 4-gate exchange sequences to a precision of  $10^{-4}$  in the cost function, with the corresponding maximum matrix element distance of the order of  $10^{-5}$ .

An alternative approach to finding gate sequences for local unitaries using the standard mapping from  $SU(2)$  to  $SO(3)$  and a quaternion representation of  $SO(3)$  can be found in Ref. [18].

Table 2 shows the gate times for each of the 4 exchange interactions required to implement the encoded local unitary operations. Note that the exchange interactions implementing  $U_1$  and  $U_2$  can be applied in parallel, as can those for  $V_1$  and  $V_2$ . Thus, transforming the 34-gate sequence of Fig. 3 into the exact *CNOT* gate on the computational basis requires 16 additional nearest-neighbor interactions, that can be realized as 8 additional parallel gate cycles.



Exchange Time	Qubit 1	Qubit 2	U1 Times	U2 Times	V1 Times	V2 Times
$t_1$	1	2	2.218823	1.391831	4.865658	0.933012
$t_2$	2	3	4.386508	1.977325	3.141319	2.025429
$t_3$	1	2	3.442139	2.974488	1.493938	1.315318
$t_4$	2	3	1.808165	2.105277	3.141314	0.042865

TABLE 2. The exchange gates and corresponding gate times (in units of  $2\hbar/J$ ) required to transform  $W$  into the actual  $CNOT$  gate.

The total number of nearest neighbor interactions for the exact  $CNOT$  amounts to 27 if applied in parallel and 50 if applied serially.

## 5. GATE SEQUENCES FOR THE THREE-QUBIT ENCODING

A 19 exchange gate sequence for a gate locally equivalent to  $CNOT$  for the three qubit encoding has been given in [16]. The layout in [16] obeyed certain symmetry constraints. We have recalculated this sequence to a higher accuracy with and without these symmetry constraints and have also computed the exchange-only implementation of the local unitaries  $U_i, V_i$ ,  $i = 1, 2$ , needed to transform the 19-gate sequence to the exact  $CNOT$  in the computational basis. The resulting sequences for exact  $CNOT$  in the three-qubit encoding are given in Appendix C.

## 6. CONCLUSION

We have presented an exact construction of a discrete universal logical gate-set using only the exchange operation with a four-qubit encoding. These results are readily applicable to physical implementation schemes in which exchange interactions are favored. These include the classical solid-state nuclear-spin qubit model proposed by Kane [24, 25] and the electron-spin qubit proposal of Loss and DiVincenzo [7, 8]. For a four-fold increase in the number of system qubits and a twenty-nine-fold increase in the number of computational cycles for the two-qubit operation, we are able to simplify the implementation of spin coupled solid state systems by entirely eliminating the need for single-spin  $A$ -gates. In contrast to the rapid and relatively easily-tunable two-spin  $J$ -gates, the  $A$ -gates demand considerably greater device complexity and  $g$ -factor engineering on solid-state heterostructures [10, 9].

Thus far, explicit constructions of universal logical gate-sets for exchange-only quantum circuits have been given on three-qubit encodings [16] and for the four-qubit scheme presented here. It should be noted that in principle the overhead in spatial resources can be made arbitrarily small: asymptotically the rate of encoding into subsystems converges to unity [14]. However we have to carefully evaluate the trade-offs in space and time for each encoding. So far no constructive analytical methods to lower bound the number of nearest neighbor interactions for encoded gates exist. Using numerical methods yields an increase from 19 to 34 gates for a gate equivalent to the encoded  $CNOT$  going from a three-qubit [16] to the present four-qubit encoding. This seems to indicate that the rate of growth of the number of nearest neighbor gates needed is rather large and that it is probably wise to stick

to small encodings if the error correcting properties are not also to be incorporated. However, we note that these are all numerical solutions and are not guaranteed to be optimal. It would therefore be useful to obtain analytic bounds on the minimum number of exchange gates required for encoded operations.

Another open problem is the application of encoded universality to other interactions encountered in nature and in the laboratory, to facilitate the search towards optimal physical schemes for implementation of universal quantum computation. We believe that the scheme presented here provides a step in this direction and alleviates the task of the quantum engineer working towards spin-coupled solid state quantum computation.

#### ACKNOWLEDGEMENTS

The effort of the authors is sponsored by the Defense Advanced Research Projects Agency (DARPA) and Air Force Laboratory, Air Force Materiel Command, USAF, under agreement number F30602-01-2-0524, and by DARPA and the Office of Naval Research under grant number FDN-00014-01-1-0826.

#### REFERENCES

- [1] D. P. DiVincenzo, Phys. Rev. A **51**, 1015 (1995).
- [2] D. Barenco *et al.*, Phys. Rev. A **52**, 3457 (1995), LANL preprint quant-ph/9503016.
- [3] A. Kitaev, A. Shen, and M. Vyalıy, *Classical and Quantum Computation*, No. 47 in *Graduate Series in Mathematics* (AMS, Providence, RI, 2002).
- [4] M. Nielsen and I. Chuang, *Quantum Computation and Quantum Information* (Cambridge University Press, Cambridge, UK, 2000).
- [5] P. O. Boykin *et al.*, in *Proceedings of 40th Annual Symposium on the Foundations of Computer Science (FOCS)* (IEEE Press, Los Alamitos, CA, 1999), pp. 486–494, LANL preprint quant-ph/9906054.
- [6] J. Kempe and K. Whaley, Phys. Rev. A **65** (5), 052330 (2002).
- [7] D. Loss and D. DiVincenzo, Phys. Rev. A **57**, 120 (1998).
- [8] G. Burkard, D. Loss, and D. DiVincenzo, Phys. Rev. B **59**, 2070 (1999).
- [9] D. P. DiVincenzo, G. Burkard, D. Loss, and E. V. Sukhorukov, in *Quantum Mesoscopic Phenomena and Mesoscopic Devices in Microelectronics.*, edited by I. O. Kulk and R. Ellialtıoglu (NATO Advanced Study Institute, Turkey, 1999), LANL preprint cond-mat/9911245.
- [10] R. Vrijen *et al.*, Phys. Rev. A **62**, 012306 (2000).
- [11] J. Kempe, D. Bacon, D. DiVincenzo, and K. Whaley, in *Quantum Computation and Information*, edited by R. Clark *et al.* (Rinton Press, New Jersey, 2001), Vol. 1, pp. 33–55.
- [12] D. Deutsch, A. Barenco, and A. Ekert, Proc. Roy. Soc. London Ser. A **449**, 669 (1995).
- [13] S. Lloyd, Phys. Rev. Lett. **75**, 346 (1995).
- [14] J. Kempe, D. Bacon, D. Lidar, and K. Whaley, Phys. Rev. A **63**, 042307 (2001).
- [15] D. Bacon, J. Kempe, D. Lidar, and K. Whaley, Phys. Rev. Lett. **85**, 1758 (2000), LANL preprint quant-ph/9909058.
- [16] D. P. DiVincenzo *et al.*, Nature **408**, 339 (2000).
- [17] J. Vala and K. B. Whaley, Phys. Rev. A **66**, 022304 (2002).
- [18] S. Myrgren and K. Whaley, Quantum Information Processing, in press, lanl-report quant-ph/0309051.
- [19] D. Bacon, K. Brown, and K. Whaley, Supercoherent quantum bits, 2001, LANL preprint quant-ph/0012018.
- [20] Y. Makhlin, Nonlocal properties of two-qubit gates and mixed states and optimization of quantum computations, 2000, LANL preprint quant-ph/0002045.
- [21] B. Buckles and F. Petry, *Genetic Algorithms* (IEEE Computer Society Press, Los Alamitos, CA, 1992).
- [22] J. C. Lagarias, J. A. Reeds, M. H. Wright, and P. E. Wright, SIAM J. Optim. **9**, 113 (1995).
- [23] J. Nelder and R. Mead, Computer Journal **7**, 308 (1965).
- [24] B. Kane, Nature **393**, 133 (1998).

[25] B. Kane, Silicon-based Quantum Computation, 2000, LANL preprint quant-ph/0003031.

### APPENDIX A. THE MAKHLIN INVARIANTS

We give a brief description of how to calculate the *Makhlin invariants* [20] for an encoded two-qubit operation  $W$ . These invariants characterize a two-qubit operation up to equivalence by local unitaries (see Eq. (6)).

In a first step project the physical operator  $W$  onto the logical subspace:

$$(8) \quad M = P^\dagger U_{cnot}^{exchange} P,$$

$P$  is a 256-by-4 matrix whose column vectors are the basis states  $\{|0_L 0_L\rangle, |0_L 1_L\rangle, |1_L 0_L\rangle, |1_L 1_L\rangle\}$ , and  $M$  is a matrix in  $SU(4)$ . We next transform  $M$  into the ‘‘Bell-basis’’ as  $M_B = Q^\dagger M Q$ , where

$$(9) \quad Q = \frac{1}{\sqrt{2}} \begin{pmatrix} 1 & 0 & 0 & i \\ 0 & i & 1 & 0 \\ 0 & i & -1 & 0 \\ 1 & 0 & 0 & -i \end{pmatrix}.$$

Finally, we define  $m = M_B^T M_B$ , to obtain the invariants  $M_1 = tr^2(m)/16detM$  and  $M_2 = (tr^2(m) - tr(m^2))/4detM$ . For gates that are locally equivalent to the  $CNOT$ ,  $M_1 = 0$  and  $M_2 = 1$ .

### APPENDIX B. NUMERICAL SEARCH FOR A GATE LOCALLY EQUIVALENT TO $CNOT$

To obtain a gate  $U_{cnot}^{exchange}$  which is locally equivalent to the encoded  $CNOT$ , we applied a combination of genetic algorithms and Nelder-Mead simplex searches. At the beginning of every search, we fixed a sequence of qubit pairs to be coupled with an exchange interaction, and optimized the fitness function  $\mathcal{F}$  with respect to time parameters only. No restrictions on symmetry were imposed, unlike [16] (see Appendix C). We started with a small number of couplings and incremented the number of exchange interactions after each unsuccessful attempt to find a gate equivalent to the  $CNOT$ . The final layout of the exchanges is indicated in Figure 3. We found that space generated by  $\mathcal{F}$  was sufficiently complex such that allowing the sequence of qubit-pairs to vary during the optimization only introduced unnecessary complications into the search.

Even with the incorporation of the leakage parameter  $\Lambda$  into fitness function  $\mathcal{F} = f + \Lambda$ , the large space of parameters is still marked with many local minima. Therefore, the first stage of our search was a *genetic algorithm*, whose heuristic is well-equipped to score large spaces aggressively in order to identify basins in which a global minimum may occur. Whereas algorithms based on the hill-descent heuristic often trap themselves into basins of local minima, genetic algorithms are able to traverse rapidly through regions of the space between the basins, enabling them to descend from one basin to another. The pseudocode for the genetic algorithm is as follows:

**Step 1: Initialization.** Let the initial population consisting of 60 *candidates* be defined as the set  $\mathbf{P}_t$ . Each member of  $\mathbf{P}_t$  is a 34-dimensional real-valued vector whose elements lie in the interval  $[0, 2\pi]$ . Each vector represents the *genome* of a candidate, and the  $j^{th}$  element in each vector ( a *gene*) is the time parameter for the Hamiltonian in the  $j^{th}$  exchange in a fixed sequence of qubit-pair exchanges.

**Step 2: Fitness Evaluation and Selection.** Generate the Makhlin invariants  $M_1, M_2$  and leakage parameter  $\Lambda$  for each candidate and rank the candidates according to their fitness scores  $\mathcal{F}$ . Sort the top 20 performing candidates into the *parental pool*.

**Step 3: Crossover.** Randomly pair the 20 members of the parental pool. Each parental pair generates two offspring. The first offspring is a random, pairwise convex combination of the genomes of the parental pair. Let  $\alpha$  and  $\beta$  be random real variables in the interval  $[0, 1]$ . For parents  $u$  and  $v$ , we have:

$$\begin{aligned} PARENT_u &= (\gamma_{u,1}, \dots, \gamma_{u,34}) \\ PARENT_v &= (\gamma_{v,1}, \dots, \gamma_{v,34}) \\ (10) \text{ OFFSPRING1}_{u,v} &= (\alpha\gamma_{u,1} + (1-\alpha)\gamma_{v,1}, \dots, \alpha\gamma_{u,34} + (1-\alpha)\gamma_{v,34}) \end{aligned}$$

The second offspring is a random geometric average of the genomes of the parental pair.

$$\begin{aligned} PARENT_u &= (\gamma_{u,1}, \dots, \gamma_{u,34}) \\ PARENT_v &= (\gamma_{v,1}, \dots, \gamma_{v,34}) \\ (11) \text{ OFFSPRING2}_{u,v} &= (\gamma_{u,1})^\beta (\gamma_{v,1})^{1-\beta}, \dots, (\gamma_{u,34})^\beta (\gamma_{v,34})^{1-\beta} \end{aligned}$$

Intuitively, each candidate in the population represents a point on a simplex within the search space. By taking convex combinations and geometric averages between the points, we search the face planes of the simplex.

**Step 4: Insertion.** We now construct the population of the next generation  $\mathbf{P}_{t+1}$ . The new population consists of:

- (1) The top  $(20 + M)$  candidates from  $\mathbf{P}_t$ , where  $M$  is a randomly generated integer between 0 and 20
- (2) The 20 offspring generated from the crossover step
- (3)  $(20 - M)$  new, randomly-generated candidates

The purpose in inserting new candidates during each generation is to enable the search to extract itself from local minima. If the search simplex has converged to a local minimum, the new candidates will serve as vertex points that can pull the search into more promising regions within the space.

**Step 5: Mutation.** We now subject the population to a random mutation process, where each gene (component of  $\mathbf{P}_t$ ) in each genome is perturbed to a new value within  $[0, 2\pi]$  with probability .03. It is necessary to introduce these mutations, corresponding to small steps in the search simplex, because the crossover operations tend to pass over global minima too rapidly. However, even small perturbations in the genome cause increasingly violent movements in  $\mathcal{F}$  as global minima are approached. So to balance these considerations, the top ten performers in each generation are exempted from mutations to stabilize the performance of the algorithm.

**Step 5': Exit Condition Check.** Check if the top-ranked candidate satisfies the condition  $\mathcal{F} < \epsilon$  for a sufficiently small  $\epsilon$ . If not, return to Step 2.

We ran four simultaneous genetic algorithms with four distinct, randomly-generated populations of size 60, and coordinated the search by inserting a clone of the top candidate from the population with the best top-performer into the other three populations. After 2394 generations, we obtained a candidate with error magnitudes of  $O(10^{-2})$  with respect to the Makhlin invariants and  $O(10^{-1})$  with respect

to the leakage parameter. At this point, the pace of progress in the genetic algorithm slowed down dramatically, so we used the top performer as the starting point for the second stage of our algorithm, a Nelder-Mead simplex direct search. At this point, the simplex search was considerably more robust, because the simplex heuristic enables the simplex to flex and squeeze itself through narrow valleys of the space more sensitively. After 5296 iterations of the simplex search, we obtained a candidate with error magnitudes of  $O(10^{-6})$  with respect to the Makhlin invariants and  $O(10^{-2})$  with respect to the leakage parameter. Since this was the first time we had advanced to such a low point in the space, we ran the genetic algorithm again to see if any further improvement could be obtained in this manner, and to acquire some further intuition about the structure of the space. After 471 generations, only a trivial improvement was obtained, so we returned to the simplex method once more. After 22081 iterations of the simplex search, we obtained error magnitudes of  $O(10^{-10})$  with respect to the Makhlin invariants and  $O(10^{-8})$  with respect to the leakage parameter.

### APPENDIX C. GATE SEQUENCES FOR $CNOT$ WITH THE THREE-QUBIT ENCODING

In Ref. [16], a numerical search was utilized to generate a  $CNOT$  gate from a sequence of nearest-neighbor exchange interactions on a system of two computational qubits, each encoded by three physical spin-1/2 qubits. The three-qubit encoding is

$$(12) \quad \begin{aligned} |0_L\rangle &= \frac{1}{2}|S\rangle \otimes |1\rangle \\ |1_L\rangle &= \sqrt{\frac{2}{3}}|T_+\rangle \otimes |0\rangle - \frac{1}{\sqrt{3}}|T_0\rangle \otimes |1\rangle, \end{aligned}$$

where  $|S\rangle = \frac{1}{\sqrt{2}}(|10\rangle - |01\rangle)$ ,  $|T_+\rangle = |11\rangle$  and  $|T_0\rangle = \frac{1}{\sqrt{2}}(|10\rangle + |01\rangle)$ . The numerical search was made by minimization of a similar fitness function to that employed here, *i.e.*, including both matrix distance from  $CNOT$  and leakage penalty functions. A candidate sequence of 19 exchanges equivalent to  $CNOT$  up to local transformations on the encoded basis ( $U_{cnot}^{exchange}$ ) was obtained for a layout containing two simplifying symmetries in the exchange gate times. These symmetries are illustrated in Figure 5, with the gate switching times given in Table 3. Here we give also the exchange-only implementation of the local gates  $U_i, V_i$ ,  $i = 1, 2$  (cf. Eq. (6)), needed to convert the 19-gate sequence into the exact  $CNOT$  in the computational basis. These were obtained using the same procedures as described in Section 4 and Ref. [18].

The first symmetry is that certain gate times are repeated in a spatially symmetric configuration, *e.g.*,  $t_4$  occurs at the beginning and end of the sequence between physical qubits 3 and 4 in each case. We denote this the *repetition symmetry*. A second symmetry apparent in Figure 5 is that certain sequential pairs of interaction times are related by analytic functions. In particular, for  $k = 5, 6, 8, 10$ , the functions

$$(13) \quad c_k = \tan(t_k)\tan(\bar{t}_k) + 2$$

are exactly equal to zero. We denote this symmetry a *correlation symmetry*. With these symmetry restrictions the optimal solution for a 19 exchange gate sequence obtained in Ref [16] yields a Makhlin invariant fitness value of  $f$  on the order of

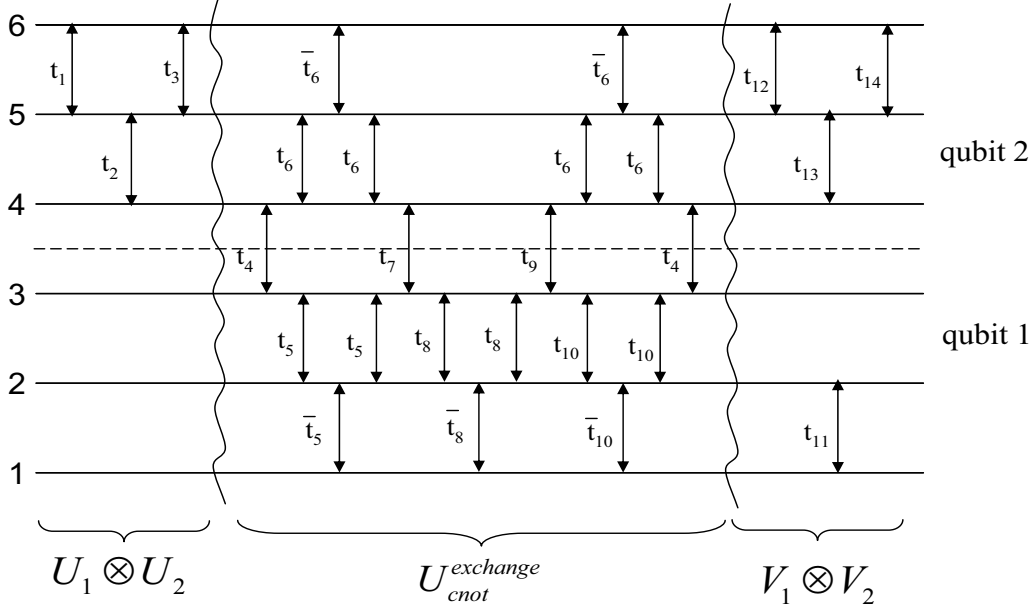


FIGURE 5. Layout for the exact  $CNOT$ . The 19-gate sequence for a gate  $U_{cnot}^{exchange}$  locally equivalent to  $CNOT$  ( $t_4 - t_{10}, \bar{t}_5 - \bar{t}_{10}$ ) is taken from Ref. [16] (time indices are shifted by three). Gate switching times are given in Table 3.

Exchange Time	Qubit 1	Qubit 2	Times	Exchange Time	Qubit 1	Qubit 2	Times
$t_1$	5	6	0.863060	$t_8$	2	3	1.302881
$t_2$	4	5	0.303496	$t_9$	3	4	0.463869
$t_3$	5	6	0.863060	$t_{10}$	2	3	2.554511
$t_4$	3	4	1.290877	$\bar{t}_6$	4	5	0.871873
$t_5$	2	3	0.650655	$\bar{t}_{10}$	1	2	1.249644
$t_6$	4	5	0.871873	$\bar{t}_6$	5	6	-1.034121
$\bar{t}_5$	1	2	-1.207108	$t_{10}$	2	3	2.554511
$\bar{t}_6$	5	6	-1.034121	$t_6$	4	5	0.871873
$t_5$	2	3	0.650655	$t_4$	3	4	1.290877
$t_6$	4	5	0.871873	$t_{11}$	1	2	0.612497
$t_7$	3	4	2.012205	$t_{12}$	5	6	2.826113
$t_8$	2	3	1.302881	$t_{13}$	4	5	2.838096
$\bar{t}_8$	1	2	-0.502098	$t_{14}$	5	6	2.278532

TABLE 3. Gate switching times for the 26 gate sequence of Figure 5, given in units of  $2\hbar/J$ . This corresponds to  $\pi$  times the time units employed in Ref. [16].

$10^{-10}$  and a leakage parameter  $\Lambda$  on the order of  $10^{-8}$ . The overall precision of the sequence, given by the maximum matrix element distance to the  $CNOT$  in the computational basis is of order  $10^{-6}$ .

We have performed a new set of numerical searches for this same 19-exchange gate layout in the three-qubit encoding, using the techniques described in this paper and without imposing any symmetry constraints on the exchange times. We find that not only can higher quality numerical solutions be obtained, but also that these are very significantly improved when the simplifying symmetry constraints are lifted. This results in a larger set of independent variables (19 instead of the 7 given in Ref. [16]) but with the advantage of a considerably smaller value of the cost function.

We performed a search with a Nelder-Mead simplex algorithm whose optimization criterion was the minimization of the Makhlin fitness function  $f$  and the leakage parameter  $\Lambda$ , starting with a random initial set of exchange gate times. Figure 6 and Table 4 shows the corresponding exchange sequence, together with the exchange-only implementation of the local gates  $U_i, V_i, i = 1, 2$  needed to convert the 19-gate sequence into the exact  $CNOT$  in the computational basis. This search yielded zero values of Makhlin fitness function  $f$  and leakage parameter  $\Lambda$  to within machine precision ( $10^{-16}$ ), and a maximum matrix element distance from the exact  $CNOT$  of  $10^{-9}$ . This provides a significant improvement over the corresponding overall precision of  $10^{-6}$  for the original 19-gate sequence of Ref. [16].

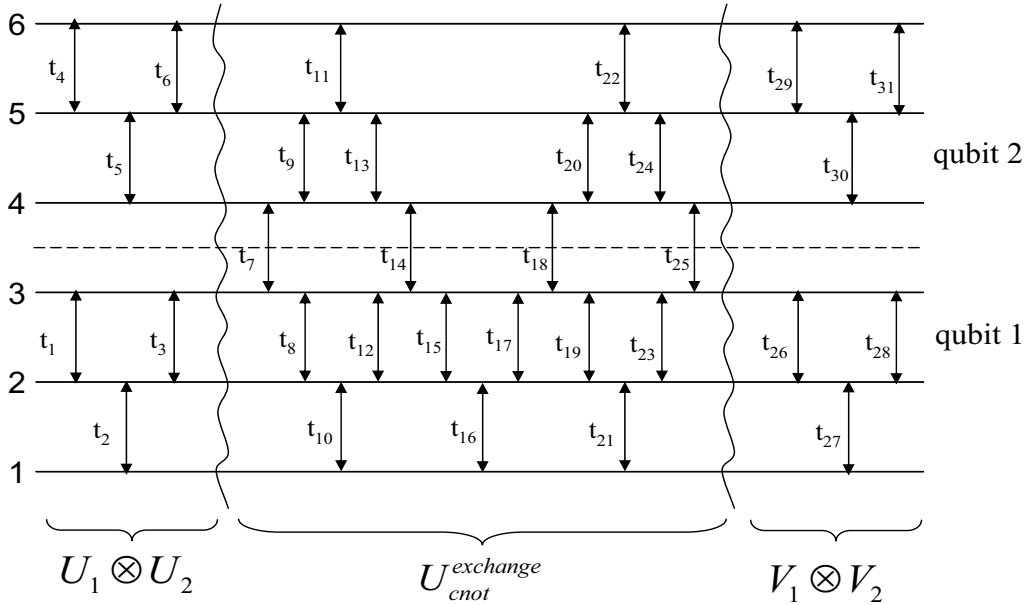


FIGURE 6. Layout for the exact  $CNOT$  obtained by unrestricted optimization of times  $t_7 - t_{25}$  for  $U_{cnot}^{exchange}$  and of  $t_1 - t_6$  and  $t_{26} - t_{31}$  for the local unitaries  $U_i, V_i, i = 1, 2$ . Gate switching times are given in Table 4.

In the solution described in [16], the correlation symmetries were satisfied to machine precision, while the repetition symmetries satisfied exactly. We note that these correlation and repetition symmetries are not essential to the task of implementing the encoded  $CNOT$  operation. From an optimization perspective, they

Exchange Time	Qubit 1	Qubit 2	Times	Exchange Time	Qubit 1	Qubit 2	Time
$t_1$	2	3	3.141592	$t_{17}$	2	3	4.444461
$t_2$	1	2	0.989737	$t_{18}$	3	4	0.463873
$t_3$	2	3	3.141593	$t_{19}$	2	3	1.249608
$t_4$	5	6	2.477807	$t_{20}$	4	5	5.249065
$t_5$	4	5	0.303496	$t_{21}$	1	2	2.554454
$t_6$	5	6	0.863060	$t_{22}$	5	6	4.013466
$t_7$	3	4	4.432470	$t_{23}$	2	3	4.391200
$t_8$	2	3	3.792238	$t_{24}$	4	5	2.107472
$t_9$	4	5	2.107472	$t_{25}$	3	4	1.290877
$t_{10}$	1	2	5.076069	$t_{26}$	2	3	3.141592
$t_{11}$	5	6	0.871873	$t_{27}$	1	2	0.927636
$t_{12}$	2	3	3.792237	$t_{28}$	2	3	3.141592
$t_{13}$	4	5	5.249065	$t_{29}$	5	6	0.863060
$t_{14}$	3	4	5.153789	$t_{30}$	4	5	0.303496
$t_{15}$	2	3	1.302870	$t_{31}$	5	6	0.466283
$t_{16}$	1	2	5.781068				

TABLE 4. Gate switching times for the 31 gate sequence of Figure 6, given in units of  $2\hbar/J$ .

might even be interpreted as a hindrance that constrains the trajectory of numerical searches to lie in sub-optimal subspaces of the control parameter space. It is not clear whether the symmetries in the solution obtained in Ref. [16] suggest the existence of analytical solutions to the optimization problem of the cost function, and if so whether these correspond to local or global minima. The above example shows that, without any symmetry restrictions and allowing the number of independent time parameters to increase, improvement to optimization of the cost function to within machine precision can be obtained.

<sup>1</sup> DEPARTMENT OF CHEMISTRY, <sup>2</sup> COMPUTER SCIENCE DIVISION, UNIVERSITY OF CALIFORNIA, BERKELEY, <sup>3</sup> CNRS-LRI, UMR 8623, UNIVERSITÉ DE PARIS-SUD, 91405 ORSAY, FRANCE